

Ordered phase and phase transitions in the three-dimensional generalized six-state clock model

Norikazu Todoroki, Yohtaro Ueno, and Seiji Miyashita

*Department of Applied Physics, University of Tokyo, Bunkyo-ku, Hongo, Tokyo 113-8656, Japan
and Department of Physics, Tokyo Institute of Technology, Oh-okayama, Meguro, Tokyo 152-8551, Japan*

(Received 14 June 2001; revised manuscript received 29 July 2002; published 6 December 2002)

We study the three-dimensional generalized six-state clock model at values of the energy parameters at which the system is considered to have the same behavior as the stacked triangular antiferromagnetic Ising model and the three-state antiferromagnetic Potts model. First, we investigate ordered phases by using the Monte Carlo twist method (MCTM). We confirmed the existence of an incompletely ordered phase (IOP1) at intermediate temperature, besides the completely ordered phase at low temperature. In this intermediate phase, two neighboring states of the six-state model mix, while one of them is selected in the low-temperature phase. We examine the fluctuation the mixing rate of the two states in IOP1 and clarify that the mixing rate is very stable around 1:1. The high-temperature phase transition is investigated by using a nonequilibrium relaxation method. We estimate the critical exponents $\beta=0.34(1)$ and $\nu=0.66(4)$. These values are consistent with the 3D-XY universality class. The low temperature phase transition is found to be of first-order by using MCTM and finite-size-scaling analyses.

DOI: 10.1103/PhysRevB.66.214405

PACS number(s): 75.10.Hk, 75.40.Cx, 75.40.Mg, 75.50.Gg

I. INTRODUCTION

The systems of Z_6 symmetry in the three dimensions (3D) have attracted interest because of their peculiar nature of orderings. In particular, there have been many works on the nature of intermediate-temperature phases.

In two dimensions, the six-state clock model shows three phases. At intermediate temperature, the discreteness of the six states is irrelevant and the system shows the same properties as that of the XY model, which is the Kosterlitz-Thouless phase where long-range order does not exist but the correlation length of the order diverges.^{1,2}

In three dimensions, the six-state clock model has also shown characteristics which are similar to the ordered phase of the XY model. However, it found that there exists only a phase where one of the six states of the model is chosen as the long-range order.³ The apparent behavior is due to the large fluctuation at the higher-temperature region of the ordered phase. However, if we generalize the energy structure of the model, a new type of intermediate phase appears.

Ueno and Kasono have introduced three-dimensional generalized six-state clock model (3D-6GCL model).⁴ The 3D-6GCL model can be regarded as prototypes of wide range of Z_6 models. That is, it represents various categories of Z_6 models according to the values of the energy parameters of the model. The existence of an intermediate phase has attracted interest for the following models: the three-dimensional three-state antiferromagnetic Potts model (3D-3AFP model) (Ref. 5), and the stacked triangular antiferromagnetic Ising model (STAFI model).⁶ Although the existence of various types of intermediate phases for these models has been proposed, there is no general understanding of the nature of the intermediate phase(s).³⁻¹² If we consider only one universality class for models with Z_6 symmetry, we conclude that the intermediate phase is an apparent phase as we found in the regular six-state model. However, it has been clarified that the situation is not so simple and an interesting new type of phase exists in the generalized case. In fact, the

3D-6GCL model was introduced in order to understand general properties of other Z_6 models.⁴ In the present paper, we study the 3D-6GCL model with a set of the parameters which is considered to correspond to the STAFI model and the 3D-3AFP model.

The Hamiltonian of the 3D-6GCL model is given by

$$\mathcal{H} = \sum_{\langle i,j \rangle} \varepsilon_0 \delta_{n_i n_j} + \varepsilon_1 \delta_{n_i n_j \pm 1} + \varepsilon_2 \delta_{n_i n_j \pm 2} + \varepsilon_3 \delta_{n_i n_j \pm 3}, \quad (1)$$

where $\langle i,j \rangle$ runs over nearest-neighbor pairs, and n_i is the spin variable which takes one of $1, 2, \dots, 6$. We set $\varepsilon_0 = 0 \geq \varepsilon_1 \geq \varepsilon_2 \geq \varepsilon_3$ as in Fig. 1. Namely, we only study ferromagnetic cases where all spins occupy the same state in the ground state. We expect that this ferromagnetic ordered phase appears at low temperature. This ordered phase is called a completely ordered phase (COP). Since the COP has six degenerate states, the order parameter space of this model is illustrated by a hexagon as in Fig. 2. The bold solid line represents one of the six COP states. The dotted line represents a mixture of neighboring two COP states which is a candidate of an intermediate phase, which we call an incom-

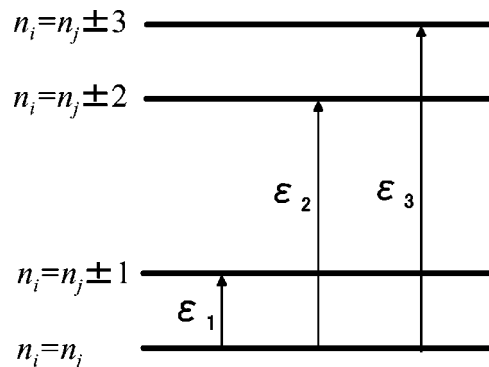


FIG. 1. Energy level of a neighboring spin pair of the 6GCL model.

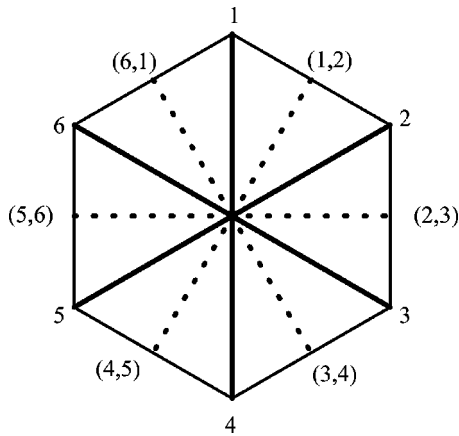


FIG. 2. Order parameter space in the 3D-6GCL model. The solid line connecting a vertex and the center is one of six low-temperature states and the dotted line between the neighboring solid lines is one of six IOP1 states.

pletely ordered phase (IOP1). As to the distribution of the spin state in the incompletely ordered phase, there have been proposed the two kinds depicted in Fig. 3. The IOP1 discussed above corresponds to Fig. 3(a). The type of Fig. 3(b) was called IOP2 which was one of the possible mixed states. For $\varepsilon_1=0$, the COP does not appear because the ground state is macroscopically degenerate. This degenerate state is IOP1 and corresponds to the ground state of the 3AFP model. Taking the approach of physical percolation to phase transitions, Ueno rigorously proved that for $\varepsilon_1=0$, at least one kind of IOP can exist at $T < \varepsilon_2 = \varepsilon_3$.¹³ For $\varepsilon_1 > 0$, Ueno and Kasono proposed that this model has two incompletely ordered phases (IOP1, IOP2) besides the COP by using the Monte Carlo twist method (MCTM).⁴ In this paper, we reexamine the nature of the intermediate phase(s) in detail.

For the 3D-3AFP model, so far various types of phases at intermediate temperatures have been proposed in previous studies, such as the permutationally symmetric sublattice phase (PSS phase) which corresponds the IOP2 (Refs. 7 and 8) or the gapless phase which is similar to the ordered phase of the three-dimensional XY model which we call the XY phase.⁹ Recent theoretical and numerical studies of the 3D-3AFP model have revealed that the existence of these phases is fake owing to the finite-size effect.¹⁴⁻¹⁶ There is only a low-temperature phase that corresponds to the IOP1.

We will show that the correlation length of the fluctuation of the order parameter in IOP1 is finite. However, the correlation length just below the critical point is so long that the

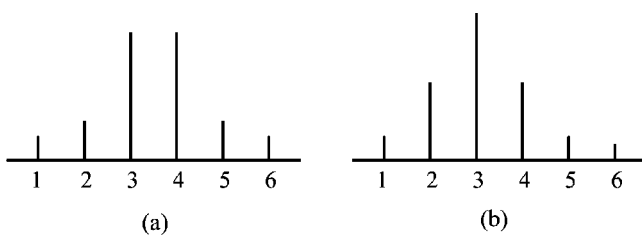


FIG. 3. Schematic of the one-spin distribution functions for two kinds of IOP's: (a) IOP1 and (b) IOP2.

phase looks like the ordered phase of the 3D XY model where the correlation length is infinite although long-range order exists. In order to distinguish the difference between the XY phase and IOP1 we have to be careful in the examination of properties of the phase.

In this paper, we study a 3D-6GCL model by using a Monte Carlo simulation and clarify properties of the phase at intermediate temperature and the nature of the phase transitions. In this study, we choose the energy parameters of the 3D-6GCL model as $\varepsilon_0=0$, $\varepsilon_1=0.1$, and $\varepsilon_2=\varepsilon_3=1.0$ which are the same as those in Ref. 4.

In order to examine the possibility of many ordered phases by the MCTM, one needs a full set of appropriate boundary conditions which cause different types of domain walls and calculate the size dependence of the excess free energy. In the present study, we deny the existence of the IOP2 as an intermediate phase from the dependence of the excess free energy on the boundary conditions. The intermediate phase shows the apparent property of the XY phase where Z_6 discreteness is irrelevant. However, we also deny the existence of the XY phase in the thermodynamic limit. This apparent property is attributed to the long correlation length at the high-temperature region of the intermediate phase. Finally, we conclude that only IOP1 exists as the intermediate temperature. The appearance of the fake XY phase near the critical point has been also found in the six-state clock model, where the Z_6 discreteness is very weak in the ordered phase near the critical point. However, the Z_6 discreteness is always relevant in the ordered phase.³

Moreover, we examine the properties of the phase transitions. We consider that the high-temperature phase transition belongs to the 3D- XY universality class. In order to confirm whether this transition belongs to the 3D- XY universality class, we study this transition by using the nonequilibrium relaxation method (NERM) and estimate the critical temperature and critical exponents. Ueno and Kasono pointed out that the low-temperature transition between the IOP1 and COP is of first order because the two phases have no symmetry relation of group and subgroup.⁴ We investigate this phase transition by using the MCTM and the usual finite-size scaling analysis, and confirm that it is of first order.

The outline of this paper is as follows. In Sec. II, we study properties of the intermediate phase. In Sec. III, we study the high-temperature transition, and in Sec. IV we investigate the low-temperature phase transition. Section V is a summary and discussion.

II. INTERMEDIATE PHASE

The properties of the phases of the 3D-6GCL model have been studied by the MCTM,⁴ which is a simulation method under special boundary conditions to detect the domain-wall excess free energy. We prepare systems with fixed boundaries in one direction and impose a periodic boundary condition in the other directions. As a reference system, we set the same state α at the boundaries (α - α) in which we expect that the ordered phase α appears. We also prepare a system where we set the states α and β at the boundaries (α - β) in

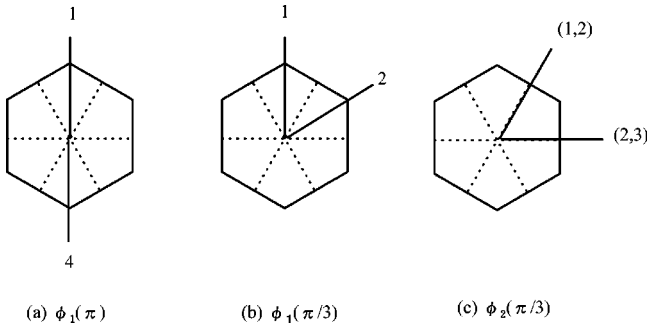


FIG. 4. Three boundary conditions for investigation of the intermediate phase by using the MCTM. (a) $\phi_1(\pi)$, (b) $\phi_1(\pi/3)$, and (c) $\phi_2(\pi/3)$.

which we expect an interface. The interfacial free energy is defined as the excess free energy between the two systems:

$$\Delta F^{\alpha\beta}(T,L) = F^{\alpha\beta}(T,L) - F^{\alpha\alpha}(T,L), \quad (2)$$

where L is a linear size of the system. Here we consider an $L \times L \times L$ system. The size dependence of $\Delta F^{\alpha\beta}(T,L)$ is given by the following asymptotic behavior for large L :

$$\psi_{\alpha\beta}(T) = \begin{cases} D-1 & \text{for a domain-wall-type interface } (\xi < \infty), \\ D-2 & \text{for a gapless interface (spin-wave type } \xi = \infty), \\ \text{noninteger} & \text{for a new type of interface.} \end{cases} \quad (4)$$

When the interface does not appear, the stiffness exponent becomes negative because $\Delta F(T,L) \rightarrow 0$ for $L \rightarrow \infty$.

In the present work, we use three sets of boundary conditions which are shown in Fig. 4. There are two kinds of boundary conditions; in ϕ_1 we fix the boundaries to be two of the low-temperature phases. The relative angle (twist angle) between the two phases can be $\pi/3$, $2\pi/3$, and π . Here we take the cases $\pi/3$ and π which are shown in Figs. 4(a) and 4(b), respectively. In ϕ_2 we fix the boundaries to be two of the IOP1's in Fig. 4(c) (twist angle $\pi/3$). As shown in Table I, we distinguish the five phases from the signs and values of the stiffness exponent. We perform MC simulations for the lattices with linear size $L = 8, 10, \text{ and } 12$ with boundary conditions $\phi_1(\pi)$, $\phi_1(\pi/3)$, and $\phi_2(\pi/3)$. At each temperature, after discarding first $5000L$, $5000L$, and $10000L$ steps, we calculate the quantities of interest using data of the

TABLE I. Values and signs of stiffness exponents for each phase.

	Disorder	IOP1	IOP2	XY	COP
$\phi_1(\pi)$	-	+	+	1	2
$\phi_1(\pi/3)$	-	-	+	1	2
$\phi_2(\pi/3)$	-	+	-	1	-

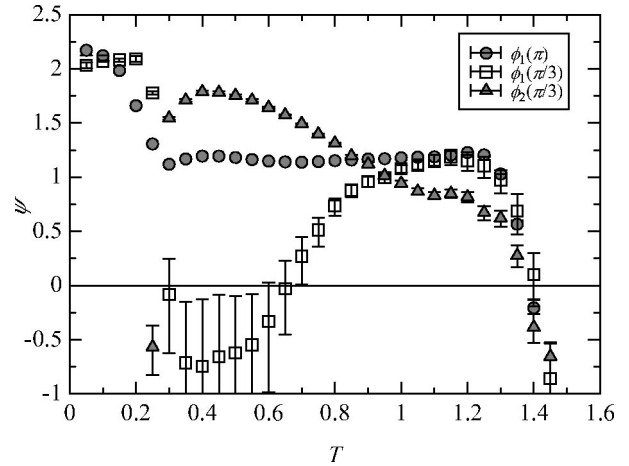


FIG. 5. Temperature dependence of the ψ under the three boundary conditions.

$$\Delta F(T,L) \sim A(\alpha,\beta)L^{\psi_{\alpha\beta}(T)}, \quad (3)$$

where $\psi_{\alpha\beta}(T)$ is called the stiffness exponent. The ordered phase is classified by the value of stiffness exponent as

next $25000L$, $25000L$, and $50000L$ steps for the three sets of boundary conditions, respectively.

In Fig. 5, we show the temperature dependence of ψ under the boundary conditions. From this figure, we may conclude the existence of the disorder phase, the XY phase, the IOP1, and the COP, as the temperature decreases. The high-temperature transition point is estimated to be $T_C \sim 1.35(5)$, and the low-temperature transition point is to be $T_F \sim 0.30(5)$. We see a change around $T \approx 0.7$ which can be a phase transition between the XY phase and IOP1.

In order to confirm the region of phases, we investigate the size dependence of the stiffness exponents for $\phi_1(\pi/3)$ for larger sizes. The region of the XY phase decreases as L becomes large (Fig. 6). The size dependence strongly suggests that the region of the XY phase disappears in the limit $L \rightarrow \infty$ and only the IOP1 exists in the intermediate-temperature region.

If we consider the domain wall between the ordered states of the type of IOP1, there is no domain wall in $\phi_1(\pi/3)$. On the other hand, one domain wall appears in the case of $\phi_2(\pi/3)$, and two domain walls appear in $\phi_1(\pi)$. Therefore, the stiffness exponent for cases $\phi_1(\pi)$ and $\phi_2(\pi/3)$ should be the same. However, we notice that the difference of the values of the stiffness exponents of $\phi_1(\pi)$ and $\phi_2(\pi/3)$ is significant at the IOP1 as we see in Fig. 5. The reason for this difference is that the effect of twisting in the system by

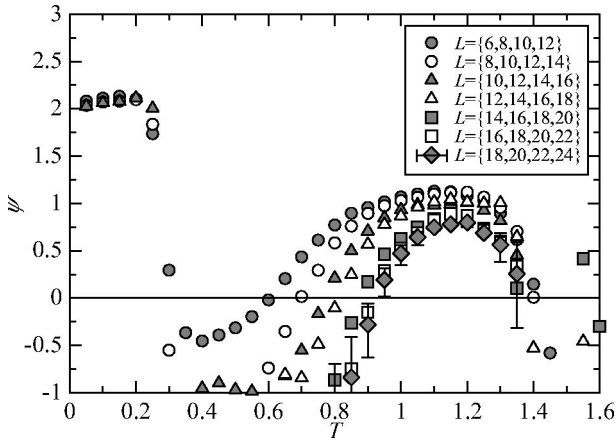


FIG. 6. Temperature and size dependence of the stiffness exponent under the boundary condition $\phi_1(\pi/3)$.

$\phi_1(\pi)$ is stronger than one of the twisting by $\phi_2(\pi/3)$. Actually, when we examine $\psi_1(\pi)$ and $\psi_2(\pi/3)$ in much larger lattice sizes, we confirm that the values of the stiffness exponents $\psi_1(\pi)$ and $\psi_2(\pi/3)$ approach the same value $\psi=2$ which indicates domain-wall-type order. In Fig. 7, we show a snapshot of the domain wall of the boundary in $\phi_2(\pi/3)$ of $L=160$ at $T=0.4$, where we find a localized domain wall clearly.

Next, following an idea of Oshikawa¹⁴ for the 3D-3AFP model, we make finite-size scaling plots of $-\langle \cos 6\theta \rangle$ by the ordinary Monte Carlo method on lattices $L=12, 18, 24$, and 30. Here, θ is the angle of magnetization from one of the COP states. After discarding the first 10 000L steps, we cal-

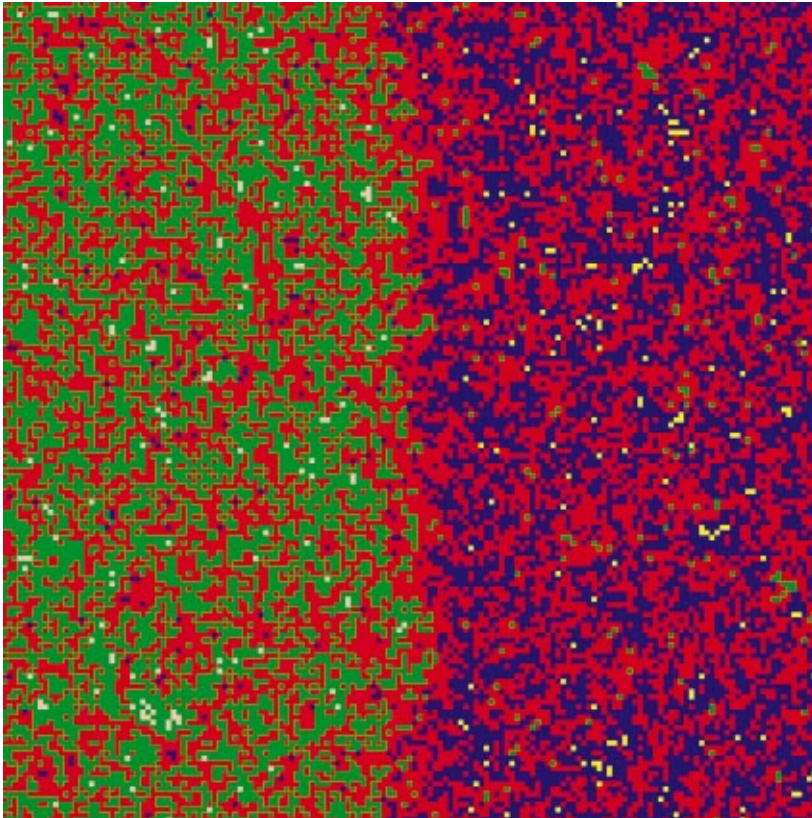


FIG. 7. (Color) Snapshot of one of the layers under the boundary condition $\phi_2(\pi/3)$ at $T=0.4$. The colors represent the states. The green cells are the state 1, the red cells are the state 2, and the blue cells are the state 3. There are some cells of different states by fluctuations.

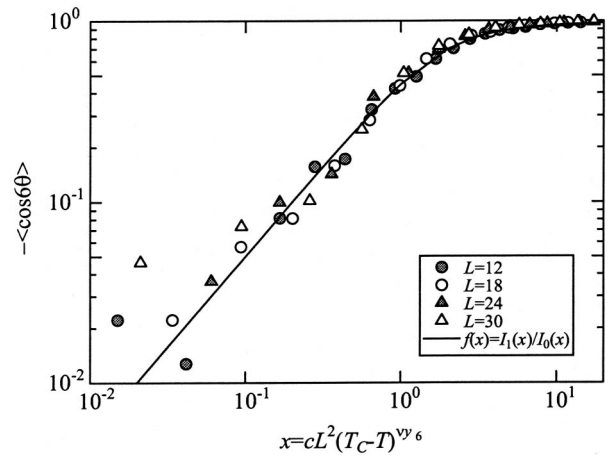
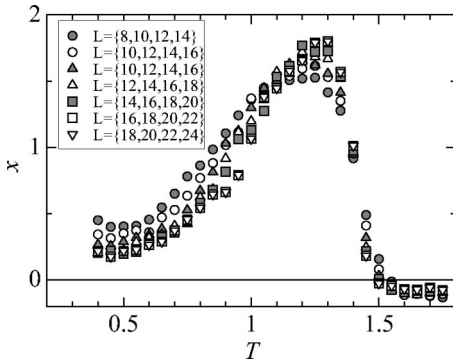


FIG. 8. Scaling plots of $-\langle \cos 6\theta \rangle$ for various system sizes and with $\nu|y_6|=3.2$ and $c=0.065$. We use $T_C=1.384$, which is estimated by using the NERM. I_n is the modified Bessel function.

culate the quantities of interest for next 40 000L steps at each temperature. In Fig. 8, we show the scaling plots in the form of the scaling function given by Oshikawa:

$$\langle \cos 6\theta \rangle \sim f(cL^2(T_C - T)^{\nu_6}). \quad (5)$$

Here, we put the value of the critical temperature $T_C = 1.384$ which was obtained by using the NERM which will be explained later. We obtain a good scaling plot when we use $\nu|y_6|=3.2$. It is important to notice here that behavior of the order in the region of the IOP1 is expressed by a scaling function using the high-temperature critical point T_C . This


 FIG. 9. Temperature and size dependence of x .

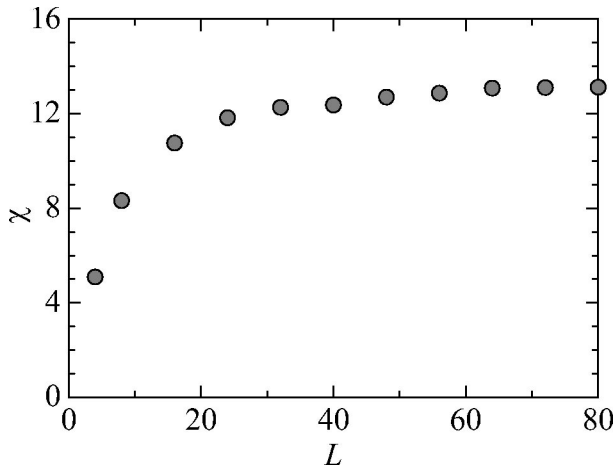
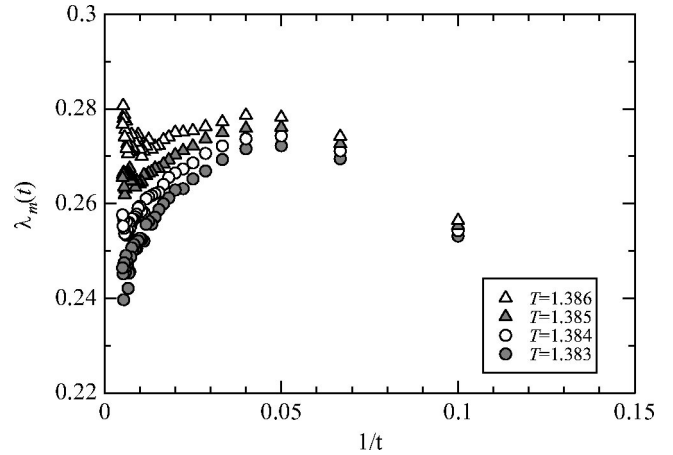
fact indicates that other phases do not exist between the IOP1 and the disordered phase. However, it is very difficult to estimate an accurate value of this exponent because the strong finite-size effect appears in the intermediate phase even in the largest system which we can calculate. After all, we conclude that the 3D-6GCL model with $\varepsilon_0=0$, $\varepsilon_1=0.1$, and $\varepsilon_2=\varepsilon_3=1.0$ has two phases, i.e., IOP1 as the intermediate phase and COP as the low-temperature phase.

In order to investigate the nature of IOP1, we examine the following quantity:

$$\chi = \frac{1}{L^3} [\langle (p_1 - p_2)^2 \rangle - \langle (p_1 - p_2) \rangle^2], \quad (6)$$

where p_i denotes the number of spin variables which take the value of the i th state. We adopt the boundary conditions $\phi_2(0)$. The asymptotical form of χ is written $\chi \sim AL^x$. The exponent x depends on the type of order. When the fluctuation is of the XY phase, we expect $x=2$. On the other hand, when the fluctuation has a finite correlation length, $x=0$.

We perform MC simulations for lattices with linear sizes $L=8, 10, \dots, 24$. For each temperature, after discarding the first $10000L$ steps, we calculate χ using data of the next $50000L$ steps. In Fig. 9, we show the size and temperature dependence of x . We find that the exponent x decreases in the IOP1 region. Moreover, we perform MC simulations for the lattice up to linear size $L=80$ at $T=0.4$ (in the IOP1 region).


 FIG. 10. Size dependence of χ at $T=0.4$.

 FIG. 11. Relaxation of $\lambda_m(t)$.

In Fig. 10, we show the temperature dependence of χ at $T=0.4$. The value of χ approaches the constant as L increases. Thus we consider that the value of x decreases and approaches 0 as $L \rightarrow \infty$, and we conclude that the fluctuation in IOP1 is the type of the domain wall and the correlation length of the fluctuation of the order parameter is finite.

III. HIGH-TEMPERATURE PHASE TRANSITION

The high-temperature phase transition in Z_6 models belongs to the 3D-XY universality class.¹⁴ Indeed, the transitions in the 3D-3AFP model¹⁵ and the six-state clock model³ are found to belong to the 3D-XY universality class. We consider that the high-temperature phase transition in the 3D-6GCL model also belongs to the 3D-XY universality class.

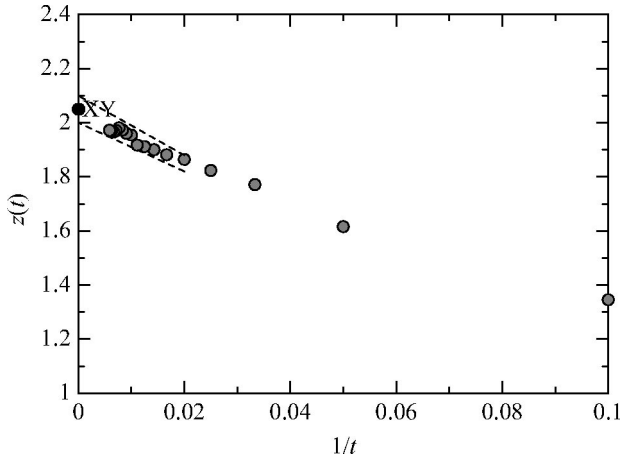
We investigate this phase transition by the NERM.¹⁷⁻¹⁹ The NERM is an efficient numerical technique to estimate the critical point and critical exponents from a dynamical process toward the equilibrium state from an ordered state. The decay of the order parameter $m(t)$ shows a power law only at the critical point. Detecting such a point, a precise determination of the critical temperature can be done. The asymptotical form of $m(t)$ at the critical temperature is written as

$$m(t) \sim t^{-\lambda_m}. \quad (7)$$

To examine asymptotic behavior of $m(t)$ clearly, we introduce a local exponent $\lambda_m(t)$:

TABLE II. Details of the simulations of NERM for the 3D-6GCL model.

Lattice size	Temperature	Monte Carlo step	Number of samples
60	1.383	200	20000
	1.384	200	60000
	1.385	200	60000
	1.386	200	20000


 FIG. 12. Relaxation of the $z(t)$ at $T_C=1.384$.

$$\lambda_m(t) \equiv - \frac{d \log_{10} m(t)}{d \log_{10} t}. \quad (8)$$

This exponent $\lambda_m(t)$ corresponds to $\beta/z\nu$. Further, we consider the following function and local exponent:

$$f_{mm}(t) \equiv \left[\frac{\langle m^2 \rangle}{\langle m \rangle^2} - 1 \right], \quad \lambda_{mm} \equiv \frac{d \log_{10} f_{mm}(t)}{d \log_{10} t}, \quad (9)$$

where $\lambda_{mm}(t)$ corresponds to d/z . Therefore, we obtain the exponents β/ν and z independently from these quantities. We simulate the relaxation process, starting from an initial state which is set to be the IOP1 state, and measure the magnetization $m(t)$. In Fig. 11, we show $\lambda_m(t)$ for the temperatures near the T_C . Here, MC simulations are performed in a lattice $L=60$. We show the MC steps (MCS) and the number of samples in Table II. The curve for $T=1.385$ turns up while the curve for $T=1.383$ turns down. Therefore we locate the transition temperature in $1.383 < T_C < 1.385$, denoting $T_C = 1.384(1)$.

At this accurate value of T_C , we calculate the relaxation of quantities. We perform about 160 000 independent runs up to 200 MCS and average the process to obtain $m(t)$. We obtain the critical exponents β/ν and z by making use of Eqs.

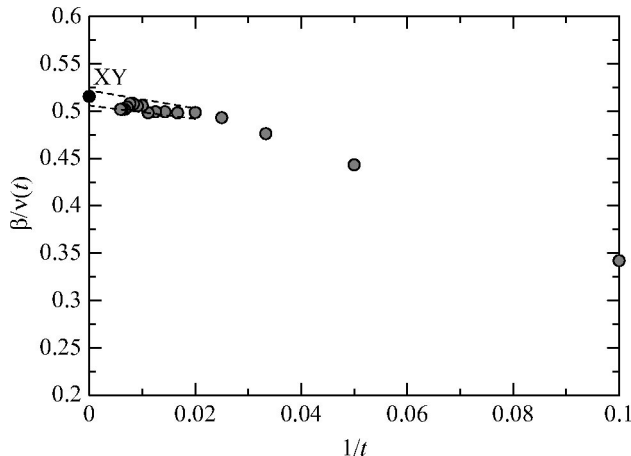
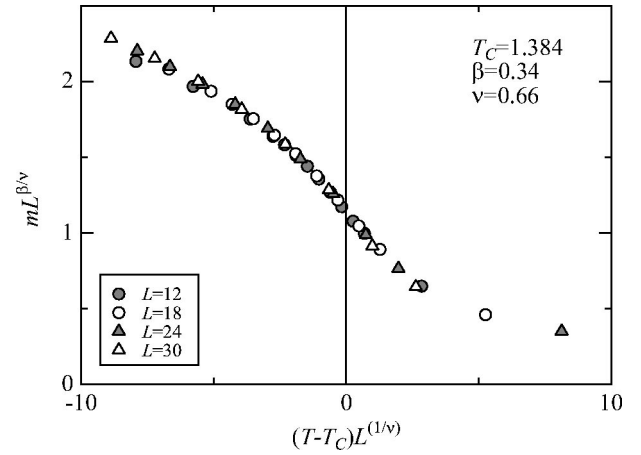

 FIG. 13. Relaxation of the $\beta/\nu(t)$ at $T_C=1.384$.


FIG. 14. Scaling plots of m for various system sizes with $\beta=0.34$, and we use $T_C=1.384$ and $\beta/\nu=0.515$, which is estimated by using the NERM.

(8) and (9). In Figs. 12 and 13, we show $z(t)$ and $\beta/\nu(t)$, respectively. From the extrapolated values of $z(t)$ and $\beta/\nu(t)$, to $1/t=0$, we estimate $z=2.05(5)$ and $\beta/\nu=0.515(10)$.

Moreover, assuming $T_C=1.384(1)$ and $\beta/\nu=0.515(10)$, we estimate β from the scaling plots of data of the magnetization which are obtained from the ordinary equilibrium MC simulation. Seeking the value of β by which the data collapse into a scaling function, we estimate $\beta=0.34(1)$ for the best fit (Fig. 14). Since the values $\beta=0.34(1)$ and $\nu=0.66(4)$ are close to the 3D-XY universality class ($\beta=0.345$, $\nu=0.669$), we conclude that this phase transition belongs to the 3D-XY universality class.

IV. LOW-TEMPERATURE PHASE TRANSITION

While many researchers have studied the high-temperature transition in the Z_6 model, few studies have been done for the low-temperature one. Ueno and Kasono pointed out that the low-temperature transition between the IOP1 and COP is of first order because they have no sym-

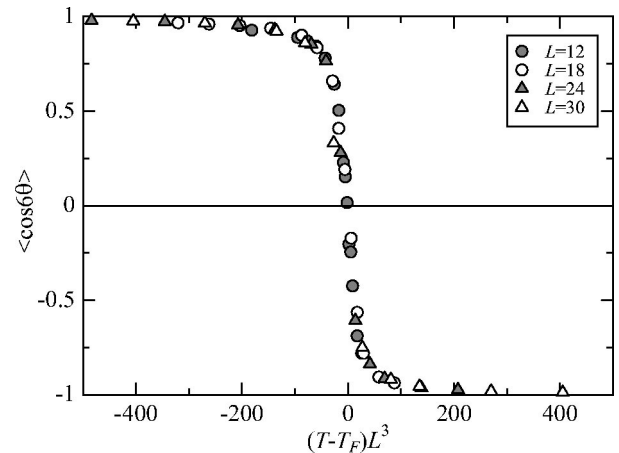


FIG. 15. Scaling plots of $\langle \cos 6\theta \rangle$ around the low-temperature phase transition with $T_F=0.295$.

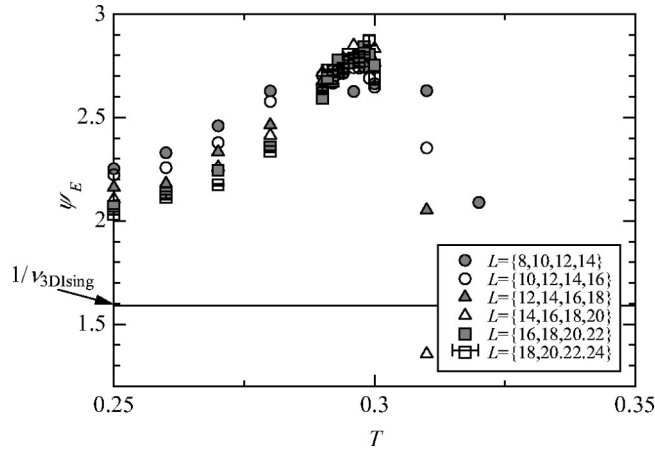


FIG. 16. Temperature and size dependence of the stiffness exponent of ΔE .

metry relation between the group and subgroup which is usually seen in the second-order transition.

In this paper we study this problem by a finite-size scaling analysis of $\langle \cos 6\theta \rangle$. If the transition is of first order, the order parameter is scaled by $\langle \cos 6\theta \rangle \sim f(\epsilon L^d)$ where $\epsilon = (T - T_C)/T_C$, d is the dimension of the system, and $f(x)$ is a finite-size scaling function. We obtain a good scaling plot at $T_F = 0.295(5)$ depicted Fig. 15. Thus we confirm this phase transition is of first order.

We also confirm this result by an analysis of extension of the MCTM.^{20,21} Now, we study the interfacial energy ΔE is defined in the same way for the excess energy due to the boundary condition causing the interface, Eq. (2). In a completely ordered phase, the size dependence of the excess energy becomes $\Delta E \sim L^{d-1}$. At the critical point, it becomes $\Delta E \sim AL^{1/\nu}$. We define the stiffness exponent of the energy ψ_E as $\Delta E \sim AL^{\psi_E}$. For the 3D Ising model at the critical point $\psi_E = 1.59$ which is considered to be a large value among 3D models exhibiting a second-order phase transition. We study ψ_E for the present phase transition. We use the boundary condition $\phi_1(\pi/3)$. In Fig. 16, we show the temperature and size dependence of ψ_E . We confirm that ψ_E approaches 3 which is much larger than the values of ψ_E of the second-order phase transition in 3D models. For the first-order phase transition, it is known that $\psi_E = D$ from the argument of wetting.²¹ This result also suggests that the present phase transition is of first order.

V. SUMMARY AND DISCUSSION

We study successive phase transitions in the 3D-6GCL model and found an intermediate phase and two phase transitions. First, it has been revealed that the intermediate phase is single phase of the IOP1. In the high-temperature region of the intermediate phase, the correlation length is very large and the system shows an apparent XY behavior. In this region the stiffness constant is very sensitive to the boundary condition. Therefore, the wrong results were obtained in previous numerical studies.⁴ The present results agree with the phase diagram of the 3D-3AFP model obtained by Kishi and Ueno and our results of the STAFI model.²² Thus, we have obtained the same intermediate phase in the three 3D Z_6 models: i.e., the 3D-6GCL model, 3D-3AFP model, and STAFI model. Moreover, we found that the mixing rate of the two states in the intermediate phase is steady and does not show anomaly fluctuation at the rate proposed previously.⁴ This IOP1 with a steady mixing of two COP states can be regarded as a partially disordered phase proposed by Mekata²³ in the original work on triangular antiferromagnets. Here we understand that the entropy effect due to the frustration allows different types of intermediate phases in two- and three-dimensional models.

Second, we examine the properties of the high-temperature phase transition, and the transition temperature is estimated to be $T_C = 1.384(1)$ with critical exponents $\beta = 0.34(1)$, $\nu = 0.66(4)$, and $z = 2.05(5)$. These values of the exponents are close to those of the 3D-XY universality class. We conclude that the universality class of this transition belongs to the 3D-XY universality class.

Third, we investigate the low-temperature phase transition in the 3D-6GCL model by using the finite-size scaling analysis and the MCTM. All of the results support that this transition is of first order. This first-order phase transition is a transition at which the $\langle \cos 6\theta \rangle$ changes from a -1 to a 1 discontinuity.

ACKNOWLEDGMENTS

We would like to thank F. Matsubara, M. Oshikawa, N. Ito, and Y. Ozeki for useful discussions. The numerical calculations were performed on the supercomputers in the Computer Center of the University of Tokyo.

¹J.L. Cardy, J. Phys. A **26**, 6201 (1982).

²D. Nelson, in *Phase Transitions and Critical Phenomena*, edited by C. Domb and J. L. Lebowitz (Academic Press, London, 1983), Vol. 7.

³S. Miyashita, J. Phys. Soc. Jpn. **66**, 3411 (1997).

⁴Y. Ueno and K. Kasono, Phys. Rev. B **48**, 16471 (1993).

⁵A.N. Berker and L. Kadanoff, J. Phys. A **13**, L259 (1980).

⁶F. Matsubara and S. Inawashiro, J. Phys. Soc. Jpn. **53**, 4373 (1984).

⁷A. Rosengren and S. Lapinskas, Phys. Rev. Lett. **71**, 165 (1993).

⁸S. Lapinskas and A. Rosengren, Phys. Rev. B **49**, 15190 (1994).

⁹R.K. Heilmann, J.-S. Wang, and R.H. Swendsen, Phys. Rev. B **53**, 2210 (1996).

¹⁰M. Kolesik and M. Suzuki, J. Phys. A **28**, 6543 (1995).

¹¹P.J. Kundrotas, S. Lapinskas, and A. Rosengren, Phys. Rev. B **52**, 9166 (1995).

¹²O. Koseki and F. Matsubara, J. Phys. Soc. Jpn. **69**, 1202 (2000).

¹³Y. Ueno, J. Stat. Phys. **80**, 841 (1995).

¹⁴M. Oshikawa, Phys. Rev. B **61**, 3430 (2000).

¹⁵Y. Ueno and R. Kishi (unpublished).

- ¹⁶R. Kishi, Master thesis, Tokyo Institute of Technology, 1999.
- ¹⁷Y. Ozeki and N. Ito, J. Phys. Soc. Jpn. **69**, 193 (2000).
- ¹⁸N. Ito, K. Fukushima, K. Ogawa, and Y. Ozeki, J. Phys. Soc. Jpn. **69**, 1931 (2000).
- ¹⁹K. Ogawa and Y. Ozeki, J. Phys. Soc. Jpn. **69**, 2808 (2000).
- ²⁰T. Takahashi, Master thesis, Tokyo Institute of Technology, 1998.
- ²¹T. Takahashi and Y. Ueno (unpublished).
- ²²T. Todoroki, Y. Ueno, and F. Matsubara (unpublished).
- ²³M. Mekata, J. Phys. Soc. Jpn. **42**, 76 (1977)